6-22-1992

Quantitative Footprinting Analysis of the Chromomycin A 3 - D N A Interaction

Allison Stankus
Syracuse University

Jerry Goodisman
Syracuse University

James C. Dabrowiak
Syracuse University

Recommended Citation

Stankus, A., Goodisman, J., & Dabrowiak, J. C. (1992). Quantitative footprinting analysis of the chromomycin A 3-DNA interaction. Biochemistry, 31(38), 9310-9318.

Quantitative Footprinting Analysis of the Chromomycin A_3–DNA Interaction†

Allison Stankus, Jerry Goodisman,* and James C. Dabrowiak*

Department of Chemistry, Center for Science & Technology, Room 1-014, Syracuse University, Syracuse, New York 13244-4100

Received January 10, 1992; Revised Manuscript Received June 22, 1992

ABSTRACT: Chromomycin A_3 (CHR) binding to the duplex d(CAAGTCTGGCCATCAGTC)·d(GACTGATGGCCAGACTTG) has been studied using quantitative footprinting methods. Previous NMR studies indicated CHR binds as a dimer in the minor groove. Analysis of autoradiographic spot intensities derived from DNase I cleavage of the 18-mer in the presence of various amounts of CHR revealed that the drug binds as a dimer to the sequence 5′-TGGCCA-3′, 3′-ACCGGT-5′ in the 18-mer with a binding constant of $(2.7 \pm 1.4) \times 10^7$ M^{-1}. Footprinting and fluorescence data indicate that the dimerization constant for the drug in solution is $\sim 10^5$ M^{-1}. Since it has been suggested that CHR binding alters DNA to the A configuration, quantitative footprinting studies using dimethyl sulfate, which alkylates at N-7 of guanine in the major groove, were also carried out. Apparently, any drug-induced alteration in DNA structure does not affect cleavage by DMS enough to be observed by these experiments.

Chromomycin A_3 (CHR),[1] Figure 1 (top panel), is a member of the aureolic acid class of anticancer drugs, which includes olivomycin and mithramycin (Miyamoto et al., 1967; Tatsuoka et al., 1960). On the molecular level these drugs exert their cytotoxic effects by binding to DNA, thereby interrupting transcription (Baguley, 1982). The binding process is facilitated by Mg^{2+} and the interaction is believed to occur in the minor groove of DNA (Brikenshtein et al., 1983; Prasad & Nayak, 1976; Ward et al., 1965).

Chromomycin and mithramycin have been the subject of numerous footprinting studies. Van Dyke and Dervan (1983) used the chemical cleavage agent Fe-MPE to show that CHR is able to recognize guanine- and cytosine-rich sites that are at least 3 base pairs in length. The affinity of sites was found to decrease in the order 5′-GGG, AGC > GCC, CCG > AGC, TCC, GTC-3′. The sequence AGC was found to have varying affinities, indicating the importance of flanking bases or the presence of nearby bound drug molecules. Strong binding of CHR to GC-rich sites was also observed in DNase I footprinting experiments (Fox & Howarth, 1985). As well as inhibiting DNase I cleavage within a binding site, CHR was found to enhance cleavage in AT-rich regions of DNA, where no drug binding takes place. The enhancements were attributed to DNA structural variations induced by the drug in the vicinity of its binding site. The study also showed that the reaction of dimethyl sulfate at N7 of guanine located in the major groove of DNA is modified in the presence of mithramycin. This prompted the authors to suggest that the drug may be binding in the major groove of DNA.

Photofootprinting studies with UO_2^{2+} indicated that mithramycin binds to GC-rich regions of DNA (Nielsen et al., 1990). Areas surrounding drug binding sites showed enhanced cleavage, suggesting that mithramycin is able to distort local DNA structure upon binding.

Footprinting analysis of DNA fragments having $(AT)_n$ inserts (Cons & Fox, 1990) suggested that, when the inserts are adjacent to mithramycin binding sites, bound drug causes

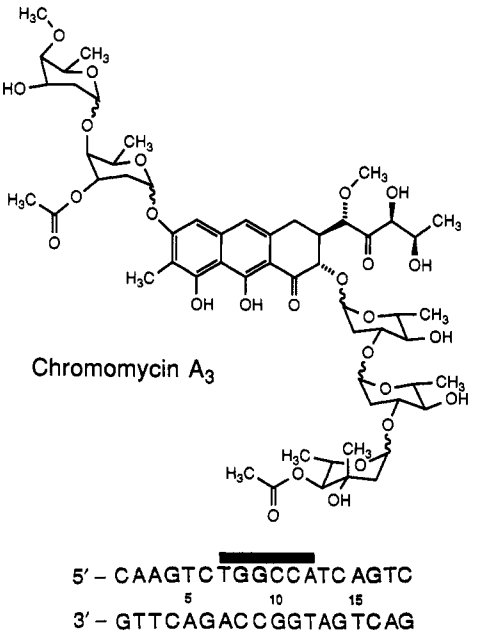

FIGURE 1: Structure of chromomycin A_3 (top) and sequence of the 18-mer with the dimer of chromomycin shown as a rectangle (bottom).

the minor groove of DNA to open, changing it to a structure which is similar to A-DNA. This conclusion was based on enhanced cleavage of DNase I, DNase II, and micrococcal nuclease at AT-rich sites adjacent to drug binding sites. All three aureolic acids, chromomycin, mithramycin, and olivomycin, have been studied using hydroxyl radical as a footprinting probe (Cons & Fox, 1989a,b). The drugs prefer to bind to the sequence GG via the minor groove of DNA.

Additional insight on the structure of the CHR–DNA complex has recently been provided by NMR. Gao and Patel (1989a,b) showed that, in the presence of Mg^{2+}, CHR binds as a symmetrical dimer to the self-complementary duplex $d[TTGGCCAA]_2$ with retention of 2-fold symmetry in the drug–DNA complex. The two CHR molecules share the minor groove at the center of the duplex in such a way that each hydrophilic edge of the chromophore is located next to a GG site. In addition, the drug-bound duplex appears to exist in the A-DNA conformation.

† We acknowledge the American Cancer Society, Grant NP-681, for support of this research.

[1] Abbreviations: CHR, chromomycin A_3; Fe-MPE, methidiumpropyl-EDTA–iron; DMS, dimethyl sulfate; TEAA, triethylammonium acetate; TE, 10 mM Tris·HCl and 1 mM EDTA, pH 7.6.

0006-2960/92/0431-9310$03.00/0

For the self-complementary duplex d[AGGATCCT]$_2$, the two preferred CHR binding sites, GG, are separated by an unpreferred site, AT. NMR studies show that, in the presence of Mg^{2+}, CHR binds as a dimer to this duplex, but the resulting drug–DNA complex does not have a C_2 symmetry axis. This suggests that binding to the preferred GG site forces half of the drug dimer to bind to the adjacent nonpreferred AT site (Gao & Patel, 1990; Leroy et al., 1991).

Other NMR investigations (Banville et al., 1990a,b) showed that both mithramycin and chromomycin bind as symmetrical dimers to the duplex d(ATGCAT)$_2$. The complexes possess C_2 symmetry, and the drug undergoes slow chemical exchange on the NMR time scale. The fact that NOE contacts exist between the sugars of the drug and several deoxyribose protons of DNA suggests that two pyranoses on one side of the aglycon are oriented along the sugar–phosphate backbone of G_3-C_4, while two other pyranoses are located near the backbone of A_5-T_6. At a molar ratio of 1 drug/duplex, mithramycin exhibits chemical exchange cross-peaks allowing an estimate of 0.4 s^{-1} to be made of its off-rate constant. Chromomycin also binds in a similar manner to the duplexes d[TATGCATA]$_2$ and d[ATAGCTAT]$_2$ but not to the duplex d[ATCGAT]$_2$ (Banville et al., 1990a). Binding takes place in a widened minor groove, in contradiction to the earlier proposed major-groove model (Keniry et al., 1987).

Although the NMR studies provide a detailed picture of the CHR–DNA complex, certain aspects of the binding mechanism remain unresolved. For example, it is not clear whether the drug binds as a preassociated dimer involving magnesium or whether it binds as a monomer, followed by cooperative binding of a second drug molecule to the adjacent DNA site. At the very low drug concentrations expected in a cell, one would expect most of the drug to be monomeric, so that monomers bound to DNA, and not dimers, would cause the cytotoxicity of chromomycin. In view of the recent interest in binding between DNA and dimers involving the aureolic acids and other agents such as distamycin (Pelton & Wemmer, 1989), we decided to study the CHR–DNA interaction using quantitative footprinting methods. Since this technique has the potential for studying binding at drug and DNA concentrations much lower than those normally used in NMR studies, it may permit observation of monomer binding to DNA.

In this report we examine the binding of chromomycin A_3 to the duplex d(CAAGTCTGGCCATCAGTC)·d(GACTGATGGCCAGACTTG), Figure 1 (bottom panel), with quantitative footprinting methods, using as probes DNase I and dimethyl sulfate (DMS). The 18-mer contains the sequence 5′-TGGCCA-3′, earlier studied by Gao and Patel (1989a,b) using NMR methods. We derive information on whether monomer or dimer is involved in the binding mechanism from the analyses of the DNase I footprinting data and fluorescence measurements on the drug and its metal complex in solution. The results of the footprinting experiments with DMS shed light on whether the drug binds to the major or minor groove and on whether bound drug induces a structural change in DNA which is detectable with dimethyl sulfate.

EXPERIMENTAL PROCEDURES

Chromomycin A_3 was purchased from Sigma and used without further purification. Solutions of the drug in ethanol were stored at 4 °C in the dark until needed. Drug concentrations were determined by UV–vis spectroscopy using the reported value of ϵ = 39 800 cm^{-1} M^{-1} at 282 nm (Van Dyke & Dervan, 1983). All other chemicals were used without further purification.

The oligomers d(CAAGTCTGGCCATCAGTC) and d(GACTGATGGCCAGACTTG) were synthesized on a 1.0-μmol scale by the DNA/Protein Core Facility, Department of Biology, Syracuse University, using standard β-cyanoethyl phosphoramidite chemistry on a DuPont Coder 300 DNA synthesizer. Typical yields were ≥50%. Each oligomer was received with the resin attached and protected at the bases and phosphate groups of DNA.

Purification of each oligomer was achieved as follows. Incubation of the sample in 1.5 mL of fresh ammonium hydroxide at 50 °C for 2 days separated the oligomer from the resin support and cleaved the β-cyanoethyl, benzoyl, and isobutyl protecting groups. Aqueous NaOH was added to a final concentration of 5 mM, and the sample was evaporated to dryness. Chromatography using a DuPont Nesorb Prep cartrigde was used to detritylate the 5′-end of each oligomer and remove salts, failure sequences, and synthetic byproducts. For this procedure the DNA was dissolved in 16 mL of 0.1 M triethylammonium acetate (TEAA), pH 7.0, and the separation was carried out on four 4-mL aliquots according to the Du Pont method. After washing of the cartridge with 10 mL of MeOH and 5 mL of 0.1 M TEAA, 4 mL of oligomer was applied to the cartridge. Subsequent washings with 10 mL of 12% CH_3CN in 0.1 M TEAA, 25 mL of 0.5% aqueous trifluoroacetic acid, and 10 mL of 0.1 M TEAA were followed by elution of the DNA in 10 1-mL fractions using 35% aqueous MeOH. Oligomer-containing fractions were identified by determining the absorbance of each solution at 260 nm. The yield of recovered product was 70%. The solvent was evaporated to dryness, and each 18-mer was reconstituted in 250 μL of TE buffer (10 mM Tris and 1 mM EDTA), pH 7.6.

To remove contaminating oligomers less than 18 base pairs in length, aliquots containing approximately 10 OD units of DNA were loaded onto a 20% polyacrylamide gel containing 6 M urea. After electrophoresis (Sambrook et al., 1989), the DNA was visualized by backshadowing the gel over a 20-cm × 20-cm Whatman PK5F silica gel plate containing a fluorescent indicator and exposing the gel to 254-nm light. Bands corresponding to the full-length oligomer were excised from the gel. DNA was recovered by crushing and soaking the polymer in TE buffer, pH 7.6, at 37 °C followed by lyophilization. Each oligomer was suspended in 6 mL of water for desalting with a Waters Sep-Pak C_{18} cartridge, and the procedure was carried out on 3-mL aliquots. After rinsing of the cartridge with 10 mL of CH_3CN and 20 mL of water, 3 mL of DNA solution was applied to the cartridge. The bound oligomer was washed with 10 mL of 25 mM aqueous ammonium bicarbonate, pH 8.0, 10 mL of 25 mM ammonium bicarbonate, pH 8.0/5% aqueous CH_3CN, and 20 mL of 5% aqueous CH_3CN. Product was recovered by elution with 12 mL of 30% aqueous CH_3CN. The collected solution was lyophilized, and each oligomer was dissolved in 300 μL of TE buffer, pH 7.6. Total product recovery was ~25%.

Solutions of double-stranded DNA were prepared by heating equimolar amounts of each single-stranded oligomer at 90 °C for 10 min and cooling slowly over 2–3 h to room temperature. Molar extinction coefficients of 168 000 cm^{-1} M^{-1} for the C-rich oligomer and 173 000 cm^{-1} M^{-1} for the G-rich oligomer were calculated from reported values for extinction coefficients of individual nucleotides and the sequence of the oligomer (Borer, 1975). All DNA solutions were stored at −20 °C. The C- and G-rich oligomers were labeled at their 5′ ends

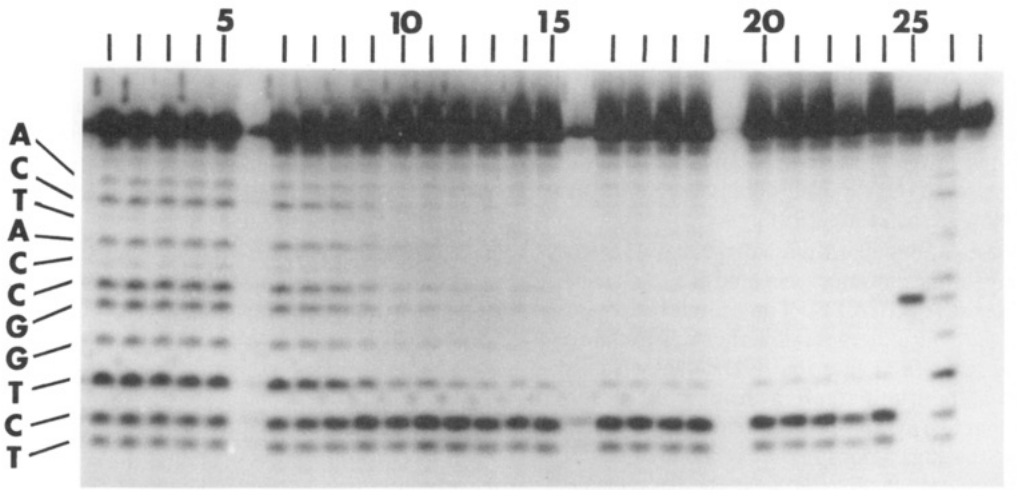

FIGURE 2: Autoradiogram showing DNase I cleavage of the 18-mer labeled at position 1 (C) in the presence and absence of chromomycin A_3. Lane 25 shows cleavage by *Hae*III, lane 26 shows cleavage by DNase I (no CHR), and lane 27 is DNA alone (no drug or enzyme). Lanes 1–15 show cleavage in the presence of increasing concentrations of CHR in the order listed in Experimental Procedures. The remaining lanes, 16–24, have CHR concentrations in the range 8.92–14.86 μM and were not used in the analysis. A partial sequence of the 18-mer is given at the left of the autoradiogram.

using [γ-^{32}P]ATP/T_4 polynucleotide kinase and purified via electrophoresis in a 20% polyacrylamide gel containing 6 M urea (Sambrook et al., 1989). Solutions of single end-labeled double-stranded oligomer with the label at position 1 (C), the C 18-mer, or position 18 (G), the G 18-mer (see Figure 1, bottom panel), were prepared by hybridizing the cold strand to the hot strand in the manner earlier described.

DNase I footprinting reactions were performed on the C 18-mer in a total volume of 12 μL, for 15 min at 37 °C, in a buffer consisting of 10 mM Tris, pH 7.6, 25% ethanol, 0.33 mM EDTA, 8 mM $MgCl_2$, and 2 mM $CaCl_2$. The footprinting experiments were performed twice. In the first experiment the final total drug concentrations present in solution were 0.15, 0.30, 0.45, 0.59, 0.74, 1.49, 2.23, 2.97, 3.72, 4.46, 5.20, 5.94, 6.69, 7.43, and 8.17 μM. In the second experiment, the concentrations were 0.1, 0.2, 0.3, 0.4, 0.5, 0.6, 0.7, 0.8, 0.9, 1.0, 1.2, 1.4, 1.6, 1.8, 2.0, 2.2, 2.4, 2.6, 2.8, 3.0, 5.0, and 10.0 μM. Drug was preincubated with DNA for 2 h at 37 °C prior to addition of the enzyme. The final concentration of DNA duplex present in all experiments was 2 μM, and the enzyme concentration was between 8×10^{-2} and 8×10^{-3} unit/μL. Assuming that all of the protein present is DNase I in the commercial preparation of the enzyme, the concentration of DNase I present in the various reactions was 10^{-7}–10^{-8} M. Reactions were quenched by addition of 6 μL of denaturing formamide loading buffer (Sambrook et al., 1989) and stored at −78 °C until the start of electrophoresis. Sequence was established by *Hae*III cleavage of the C 18-mer in a total volume of 12 μL for 1 h at 37 °C. The final concentration of DNA was 2 μM in duplex, and the *Hae*III concentration was about 0.21 unit/μL. Aliquots of reactions were heated to 90 °C and loaded onto 25% (19:1 w/w acrylamide/bisacrylamide) polyacrylamide gels containing 6 M urea. DNA fragments were separated by electrophoresis at 55 °C using an in-house-developed electrophoresis device. A Molecular Dynamics 300A computing densitometer was used to scan autoradiograms to yield whole-area spot integrations (volumes) proportional to DNA concentrations. The autoradiogram for the first footprinting experiment is shown in Figure 2. The sum of volumes of all the cleavage products as a function of drug concentration is shown in Figure 3. Individual spot intensities as a function of drug concentration (footprinting plots) are given in Figures 4 and 5. The autoradiogram for the second DNase I experiment is shown in Figure 6.

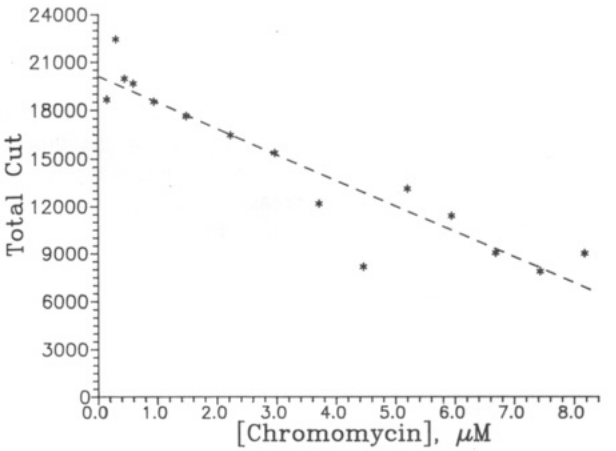

FIGURE 3: Total-cut plot for first DNase I footprinting experiment (Figure 2), with linear fit.

In separate reactions, dimethyl sulfate/piperidine footprinting studies were performed using the C 18-mer duplex labeled at C and G 18-mer duplex labeled at G. These were done in a total volume of 12 μL, for 5 min at 37 °C, in a buffer consisting of 6 mM Tris, pH 7.6, 7.5% ethanol, 0.6 mM EDTA, and 8 mM $MgCl_2$. The final drug concentrations for the studies involving the C 18-mer were 0.005, 0.01, 0.05, 0.1, 0.5, 1.0 (0.25) 5.0, 10, 15, 25, and 50 μM. The same concentrations were used for the G 18-mer. Drug was preincubated with 2 μM of duplex for 2 h at 37 °C, followed by addition of dimethyl sulfate to a final concentration of 1.7% (v/v). After incubation at 37 °C for 5 min, reactions were quenched with DMS stop solution (Sambrook et al., 1989) chilled to 0 °C. To help precipitate DNA samples during subsequent purification, 4 mg (1 mg/μL) of an aqueous solution of calf thymus DNA was added. DNA was recovered by ethanol precipitation as previously described (Sambrook et al., 1989). Dried samples were incubated in 100 μL of 1 M aqueous piperidine for 30 min at 90 °C. The reaction products were evaporated to dryness, ethanol-precipitated, and lyophilized as above. DNA was resuspended in 10 μL of denaturing formamide loading buffer, heated to 90 °C for 5 min, and electrophoresed in denaturing polyacrylamide gels as in the DNase I footprinting experiments. The resulting autoradiograms were scanned with a Molecular Dynamics densitometer.

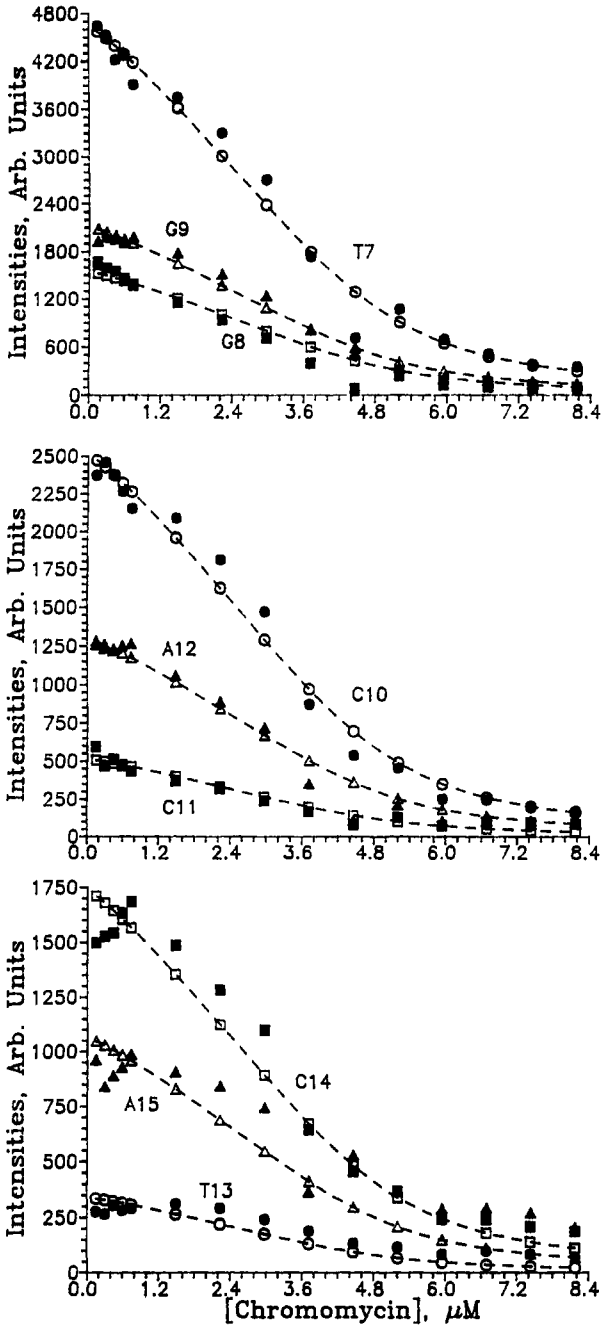

FIGURE 4: Total-cut corrected footprinting plots (solid symbols) for drug-blocked sites with theoretical fits (open symbols). Data derived from Figure 2. Model includes dimer binding and dimerization in solution.

Fluorescence spectra of chromomycin A_3 were recorded on a Hitachi F-4010 fluorescence spectrophotometer. For measurements in a solvent system consisting of 10 mM Tris buffer, pH 7.6, 0.33 mM EDTA, 8 mM $MgCl_2$, 2 mM $CaCl_2$, and 25% EtOH, emission spectra were recorded from 408 to 700 nm using an excitation wavelength of 408 nm. Spectra of drug solutions in the same solvent system, but without $MgCl_2$, were obtained in the same manner.

ANALYSIS

Establishing the Model. Examination of the experimental DNase I footprinting plots (intensity of cut fragment vs total drug concentration) showed a decrease in cutting with added drug for sites 7 through 15, ascribed to the classic footprinting phenomenon: bound drug prevents DNase I from cleaving.

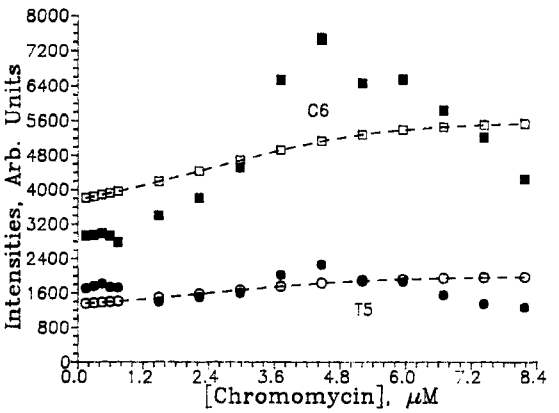

FIGURE 5: Experimental footprinting plots for cleavage of sites 5 and 6, with calculated plots (open symbols) from model including dimer binding and dimerization in solution.

The enzyme possesses a small loop which blocks cleavage about 3 base pairs to the 3′ side of a drug binding site (Suck & Oefner, 1986). Since the inhibition length is 9 base pairs long and the loop on the enzyme is ~3 base pairs, our results are consistent with a drug dimer covering the sequence 5′-TGGCCA-3′ of the 18-mer. The footprinting plots for sites 5 and 6, outside of the drug binding site, do not show inhibition. Intensities for site 5, which is farthest from the drug binding site, are roughly constant with added drug while site 6 shows a sharp increase near 3 μM drug followed by a decrease after about 5 μM. Sites 1–4 of the 18-mer are not cleaved by DNase I, because the affinity of the enzyme for the ends of DNA is low (Suck & Oefner, 1986), and sites 16–17 are weakly cleaved. Due to their low intensity and proximity of their spots to the parent band, they were not used in the analysis.

The total cut (sum of intensities for cutting at sites 5–15, and not including the parent band) for the first DNase I experiment was plotted against chromomycin concentration (Figure 3). Since most of the observed sites show decreased cleavage, the total cut I_t decreases as drug concentration increases. It is fit adequately by the linear function $I_t = 20094 - 1617[CHR]$. To correct for gel loading and other errors, all spot intensities for each drug concentration are multiplied by the ratio of I_t to the actual total cut for that concentration. With two exceptions, the correction factors differ from unity by 12% or less. The resulting intensities are shown in Figures 4 and 5. The total cut for the second footprinting experiment (Figure 6) was fit to the linear function $I_t' = 3595.4 - 239.2[CHR]$. Spot intensities for each drug concentration were corrected using I_t'. Footprinting plots (not shown) resemble those for the first experiment.

Enlightening information about binding of drug molecules to the fragment may be obtained from the initial relative slopes, calculated by fitting intensities for the first n drug concentrations to a straight line and dividing the slope by the intercept. The value of n must be large enough to give a significant variation in intensity but not so large that the footprinting intensities vary nonlinearly with drug concentration. We have tried several values of n; the conclusions drawn from the initial relative slopes are the same. Results for $n = 11$, corresponding to drug concentrations from 0.1 to 5.2 μM, are shown in Figure 7. The error bars give the uncertainty in each initial relative slope, calculated from the least-squares fit.

The cleavage inhibition for sites 7–15 is shown clearly by the negative slopes. The large drug-induced enhancement in cleavage for site 6 is evidenced by the large positive slope, while the small slope for site 5 reflects the near-constancy of the intensity for this cleavage product. Furthermore, we note

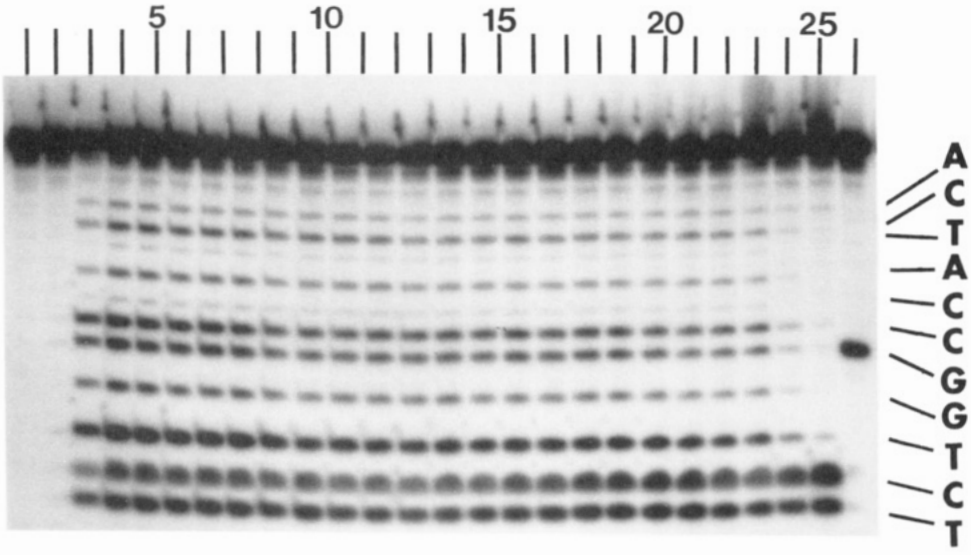

FIGURE 6: Autoradiogram for DNase I cleavage of the 18-mer labeled at position 1 (C) in the presence and absence of chromomycin A_3. Lane 26 shows cleavage by *Hae*III, lane 3 shows cleavage by DNase I (no CHR), lane 1 shows DNA alone (no drug or enzyme), and lane 2 shows DNA alone (no drug or enzyme) heated to 37 °C for a total of 2 h 15 min and then to 90 °C for 5 min according to the footprinting research protocol. Lanes 4–25 show cleavage in the presence of increasing concentrations of CHR, in the order listed in Experimental Procedures. A partial sequence of the 18-mer is given at the right.

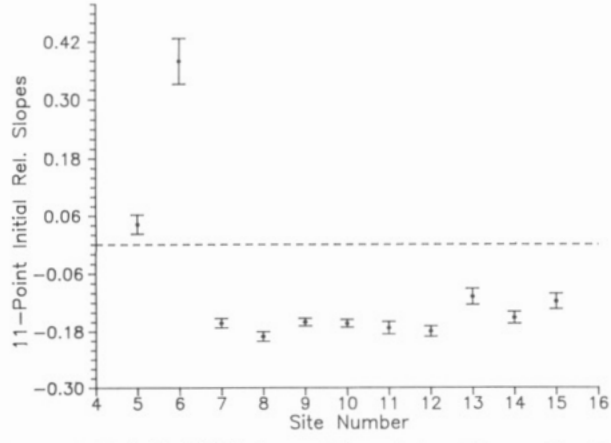

FIGURE 7: Relative initial slopes of footprinting plots as a function of sequence.

that, within the uncertainties due to the scatter in the data, the slopes may be the same for all sites in the inhibition region. The inhibition region could result from two monomer binding sites, such that a drug bound at the first blocks sites 7–12 from cleavage, including 3 base pairs for the loop on DNase I (Suck & Oefner, 1986), and a drug bound to the second blocks cleavage at sites 10–15. The fact that initial relative slopes are the same for all sites means that the binding constants are not very different for the two binding sites.

Now if there were two monomer binding sites, cleavage at positions 10–12 would be blocked by drug binding at either site, and the footprinting intensities for these cleavage sites would decrease faster with drug concentration than intensities for cleavage sites blocked by only one drug binding event. The initial relative slopes show this is not the case, and we can rule out monomeric binding of drug to the 18-mer. Calculations for models allowing for independent monomer binding bear this out: this model cannot fit the data. The sum of squared deviations between experimental and calculated intensities (D, eq 1) is greater than 5×10^6, whereas models including dimer binding (see below) give $D \sim 10^5$.

The reason that there is essentially no DNA fragment with monomer bound could be (1) unbound drug in solution exists only in the form of dimer or (2) the binding is highly cooperative. In the latter case, the binding constant of a drug molecule to DNA is much higher when the DNA has already bound one drug molecule than when no drug is bound, so it is very unlikely to find a DNA fragment with only one drug bound. This is the situation for the anticancer drug actinomycin D interacting with the duplex $[d(CGTCGACG)]_2$ (Snyder et al., 1989). To determine whether dimerization of chromomycin occurs in solution, we analyzed the footprinting intensities for sites 7–15 by a model including drug dimerization as well as drug binding.

Let $\tilde{I}_{ij}$ be the spot intensity for the ith site and the jth drug concentration as calculated from a model. $\tilde{I}_{ij}$ will depend on one or more nonlinear parameters such as equilibrium constants. The values of such parameters are obtained by minimizing the deviation between calculated and measured intensities:

$$D = \sum_{ij} (\tilde{I}_{ij} - I_{ij})^2 \qquad (1)$$

For the first data set, for which there are 15 drug concentrations and 9 sites (only the binding sites are considered), D is a sum over 135 points. The minimization of D with respect to nonlinear parameters is carried out by the Simplex procedure (Fletcher, 1980). By comparing the lowest values of D for different models applied to the same data set one can judge whether one model is significantly better than another.

The intensity for spots resulting from cleavage at site i (i = 7–15) is proportional to the probability that a duplex has no dimer bound and to the amount of available probe at the site. Since binding of drug to some duplexes prevents binding of the cleavage agent, it increases probe concentration in bulk solution and on duplexes where no drug is bound. When the rate of cleavage is limited by available probe, the cleavage may be substantially enhanced. This "mass-action enhancement" (Ward et al., 1988; Goodisman & Dabrowiak, 1992) may be taken into account by multiplying the calculated spot intensity by an enhancement factor, calculated by assuming the amount of probe bound to all DNA sites remains constant with drug concentration. This implies that the total cut does not change with drug concentration, as has been observed in numerous footprinting experiments. However, this does not

obtain in the present case, as seen in Figure 3, so the mass-action model is not usable here. Instead, we consider the probe–DNA binding equilibria explicitly, as was done previously in treating binding to a single site (Rehfuss et al., 1990).

The drug-binding equilibria that must be taken into account are the following:

$$CHR + CHR \rightleftarrows CHR_2 \quad (2)$$

$$CHR_2 + N \rightleftarrows CHR_2N \quad (3)$$

Here, CHR is unbound drug monomer, CHR_2 is unbound drug dimer, N is the 18-mer, and CHR_2N is the 18-mer duplex with bound drug dimer. The equilibrium CHR + N ⇄ CHRN is not considered, since [CHRN] is not measurable, and consideration of this equilibrium would introduce an additional equation and an additional unknown. The equilibrium between CHRN, CHR, and $CHRN_2$ is a combination of the others.

Binding of Preexisting Dimer to 18-mer. We first suppose the dimerization constant is so large that only dimer is present in solution; the binding equilibrium, eq 3, is written

$$K_1 = \frac{c_b}{c_0(N - c_b)} \quad (4)$$

where c_b is the concentration of duplexes with dimer bound, N is the total concentration of oligomers (2 μM), and c_0 is the concentration of unbound dimers. If c_t is the nominal total drug concentration, expressed as monomer

$$c_t = 2c_0 + 2c_b = 2c_0 + 2\frac{N}{1 + (K_1c_0)^{-1}} = 2c_0\left(1 + \frac{NK_1}{K_1c_0 + 1}\right) \quad (5)$$

This could be solved for c_0 for each c_t, giving the probability that a duplex has no drug dimer bound as $1 - c_b/N$.

We must also consider the probe-binding equilibrium. Suppose there are n probe sites per oligonucleotide, m of which are blocked by a bound drug dimer. The n sites include sites for which cleavage intensities are not measured (i.e., 15–17). Let ν_0 be the fraction of oligomers with neither drug nor probe bound, ν_b the fraction with drug alone bound, ν_i the fraction with a single probe molecule bound at probe site i (i = 1–n), and ν_i' the fraction with a drug dimer bound and a probe molecule bound at probe site i [$i = (m + 1)$–n]. We assume the foregoing represent all the possibilities, so that, for example, there is never more than one probe bound to a DNA fragment; therefore, $\nu_o + \nu_b + n\nu_i + (n - m)\,\nu_i' = 1$. In terms of eqs 4 and 5, $c_b = N\nu_b + (n - m)N\nu_i'$. Assuming that the binding constant for drug is the same whether or not a probe molecule is bound to the fragment (at a site from $m + 1$ to n), the equilibrium equations are

$$K_1 = \frac{N\nu_b}{N\nu_o(^1/_2c_t - N\nu_b - (n - m)N\nu_i')} = \frac{N\nu_i'}{N\nu_i(^1/_2c_t - N\nu_b - (n - m)N\nu_i')} \quad (6)$$

$$K_p = \frac{N\nu_i}{N\nu_o(P_t - Nn\nu_i - N(n - m)\nu_i')} \quad (7)$$

where K_p is the binding constant for probe and P_t is the total probe concentration. The above equations are solved to obtain ν_i and ν_i' for each value of c_t. Then, calculated intensities are

$$\tilde{I}_{ij} = A_i'\nu_i \quad (8a)$$

for i = 1–m and

$$\tilde{I}_{ij} = A_i'(\nu_i + \nu_i') \quad (8b)$$

for $i = (m + 1)$–n. The values of the linear parameters A_i', which are proportional to digest time and cutting rate constants, and thus different for different sites, are determined in the minimization of D. Sites from $m + 1$ to n will automatically show the mass-action enhancement, if it exists, since ν_i and ν_i' are calculated taking into account the probe-binding equilibrium.

The nonlinear parameters are K_1, K_p, and P_t. In principle, all could be found from the minimization of D, eq 1, but because of dependence between the parameters the data are not sufficiently precise to yield reliable values. One can estimate K_p as 2×10^4 M^{-1} (Rehfuss et al., 1990) and P_t as 1×10^{-7} M (see above) and find only K_1 by minimization of D. The resulting value of K_1 is 5.2×10^6 M^{-1}, with $D = 3.0 \times 10^6$. If P_t is fixed at 10^{-7} M and the other two parameters are varied, we find $K_1 = 7.1 \times 10^6$ M^{-1}, $K_p = 1.2 \times 10^5$ M^{-1}, and $D = 2.4 \times 10^6$. If 10^{-8} M is used for P_t, we find a minimum D of 2.3×10^6 with $K_1 = 7.1 \times 10^6$ M^{-1} and $K_p = 1.1 \times 10^5$ M^{-1}. If K_p is fixed at 2×10^4 M^{-1}, variation leads to a minimum D of 2×10^6 with $K_1 = 7 \times 10^6$ M^{-1} and $P_t = 3 \times 10^{-8}$ M. Of course, if both K_p and P_t are varied (as well as K_1) to minimize D, one can reduce D somewhat, to 1.9×10^6, but three variable parameters are now involved, and the decrease in D is insufficient to place confidence in values for all three parameters. (The values obtained are $K_1 = 7.0 \times 10^6$ M^{-1}, $K_p = 1.1 \times 10^5$ M^{-1}, and $P_t = 1.4 \times 10^{-8}$ M). Using the second data set, we find $K_1 = 2.1 \times 10^6$ M^{-1} by minimizing D, keeping $P_t = 5 \times 10^{-7}$ M and $K_p = 2 \times 10^4$ M^{-1}. Here, D is 1.55×10^5 and its value cannot be reduced much by changing the assumed values of K_p and P_t. With $P_t = 1 \times 10^{-7}$ M, the minimum D is 1.53×10^5, obtained with $K_1 = 2.0 \times 10^6$ M^{-1}.

The Drug Monomer–Dimer Association. To consider the possibility of monomers existing in solution, we introduce the equilibrium constant K_3 which describes monomer-dimer association outside of DNA, eq 2:

$$K_3 = c_0/c_m^2 \quad (9)$$

As before, c_0 is the concentration of drug dimer in solution, and c_m is the concentration of drug monomer in solution. The equilibrium between unbound drug monomer and drug monomer bound to DNA is not considered because, as shown above, bound monomer is of negligible importance. The total drug (monomer) concentration is now

$$c_t = c_m + 2c_0 + 2c_b = (c_0/K_3)^{1/2} + 2c_0 + \frac{2NK_1c_0}{K_1c_0 + 1} \quad (10)$$

This model becomes equivalent to the previous one for large K_3. Equation 10 is rewritten as

$$c_0 = \frac{c_t}{2 + (K_3c_0)^{-1/2} + 2NK_1(1 + K_1c_0)^{-1}}$$

and solved iteratively to obtain c_0 for each c_t, K_1, and K_3. Calculated spot intensities are given by eq 8.

We now minimize D, eq 1, with respect to the two nonlinear parameters, K_1 and K_3, associated with dimer binding to the 18-mer and the monomer–dimer drug association in solution, respectively. Again we take $P_t = 1.0 \times 10^{-7}$ M and $K_p = 2.0$

$\times 10^4$ M^{-1}. We find $D = 1.9 \times 10^6$, $K_1 = 3.5 \times 10^7$ M^{-1}, and $K_3 = 6.4 \times 10^4$ M^{-1}. The decrease in D from 3.0×10^6 (found assuming all drug is in the dimeric form; previous section) is large, indicating the value of K_3 is significant. For the second data set, variation of K_3 leads to a decrease in D to 1.2×10^5. To estimate errors, we find how much K_1 or K_3 must be changed to increase D by 10%. This procedure gives, for the first data set, $K_1 = (3.5 \pm 1.8) \times 10^7$ M^{-1} and $K_3 = (6.0 \pm 3.0) \times 10^4$ M^{-1}. For the second data set, this procedure gives $K_1 = (2.3 \pm 1.5) \times 10^8$ M^{-1} and $K_3 = (4.0 \pm 3.0) \times 10^3$ M^{-1}. It should be added that uncertainties in parameters are underestimated, since, if one changes K_1 and K_3 simultaneously, their values can be changed by more than the above, with only a small change in D.

The self-association constant of chromomycin, K_3, is considerably higher than that found for the anticancer drug daunomycin, $\sim 10^2$ M^{-1} (Chaires et al., 1982). However, at concentrations of <1 μM the drug exists mostly as a monomer in solution. Thus, the binding of two drugs to the 18-mer is most likely the result of the binding of one drug followed by the cooperative binding of a second drug rather than binding of a preassociated dimer to the duplex.

Analysis of the Fluorescence Data. The monomer–dimer equilibrium can be investigated by fluorescence intensity measurements. If fluorescence intensity is proportional to the nominal drug concentration (Beer's law), it is probable that only one fluorescent species is present. Deviations from Beer's law imply the presence of more than one species, such as monomers and dimers, in equilibrium with each other in solution.

Assuming an equilibrium between two monomers and a dimer, we have

$$c_t = c_m + 2c_0 \tag{11}$$

where c_t is the nominal drug concentration. Combining eq 11 with the dimerization equilibrium equation (eq 9), we can solve for c_m and c_0. Writing the fluorescence due to monomers as $a_m c_m$ and that due to dimers as $a_d c_0$, we have for the total

$$f = a_m\left(\frac{-1 + (1 + 8K_3c_t)^{1/2}}{4K_3}\right) + a_d\left(\frac{1 + 4K_3c_t - (1 + 8K_3c_t)^{1/2}}{8K_3}\right) \tag{12}$$

If $a_d = 2a_m$, f becomes just $a_m c$, independently of K_3, but if $a_d \neq 2a_m$, the deviation from linearity in a plot of f vs c yields information about K_3. If K_3 is small (no dimers) one will have $f \simeq a_m c_t$, while if $K_3 \rightarrow \infty$ (no monomers) one will have $f = a_d c_t/2$; intermediate K_3 values make f nonlinear in c_t. For small c_t, it is appropriate to expand the square roots in eq 12 as power series in c_t, giving

$$f = a_m c_t + (a_d - 2a_m)K_3 c_t^2 - 2(a_d - 2a_m)K_3^2 c_t^3 + \ldots \tag{13}$$

Thus, a fit of experimental f to a power series in c_t will permit determination of the three parameters in eq 13, a_m, a_d, and K_3. One could try to fit eq 12 directly, but one would not be able to assess the effect of increased number of terms as in the power series.

Figure 8 shows fluorescence intensities at 664.8 nm for chromomycin concentrations up to 2.8 μM in the absence of Mg^{2+} and up to 5.5 μM in the presence of 8 mM Mg^{2+}. In the latter case, the sum of the squares of residuals is 0.071, 0.031, or 0.030 for linear, quadratic, or cubic fits. Thus, the intensity is clearly nonlinear in concentration, but the cubic term is small and hence difficult to determine accurately. The

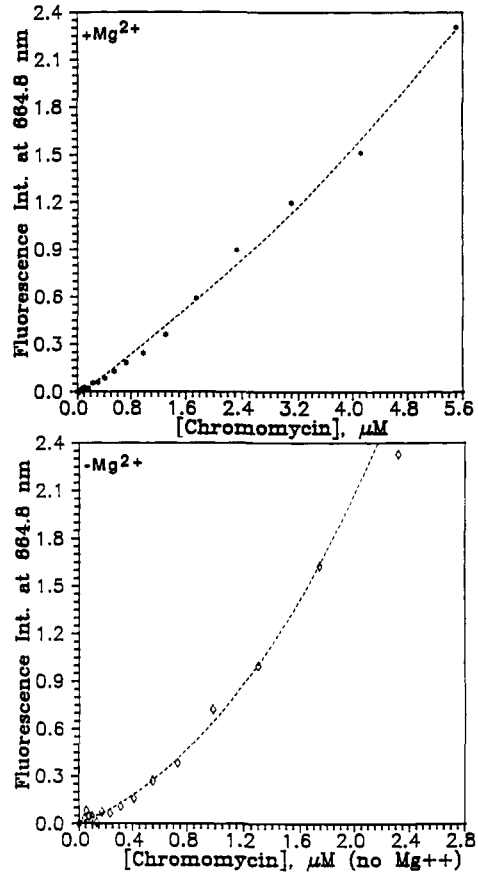

FIGURE 8: Fluorescence intensity as a function of nominal drug concentration, with and without Mg^{2+}. Cubic polynomial fits are shown.

polynomial coefficients are –0.020, 0.280, 0.0383, and –0.00241, so that, from eq 13, $-2K_3 = -0.00241/0.0383$ and $K_3 = 3.2 \times 10^4$ M^{-1}. However, the uncertainty is large: if we eliminate the data point for 5.5 μM, the sum of squares of residuals is reduced to 0.0034, suggesting that this point is in error. The coefficients are –0.005, 0.110, 0.177, and –0.0280, which makes $K_3 = 7.9 \times 10^4$ M^{-1}. This is of the same size as the value from analyses of the footprinting data.

The effects of Mg^{2+} on oligomerization of CHR in the absence of DNA have previously been studied. Hayasaka and Inoue (1969) used sedimentation equilibrium to show that, in the presence of Mg^{2+} and high (1 mM) concentration of the drug, aggregates corresponding to tetramers and pentamers formed in solution. Calcium ion, also present in the buffer used in the study, apparently has little affinity for the drug (Itzhaki et al., 1990) and does not facilitate drug binding to DNA as does Mg^{2+} (Cons & Fox, 1989a,b).

Fluorescence intensities in the absence of Mg^{2+} (lower plot of Figure 8) are analyzed in the same way. The sums of squares of residuals for linear, quadratic, and cubic fits are 0.217, 0.039, and 0.012, so the intensities are clearly nonlinear in concentration. The coefficients for the cubic fit are 0.038, –0.023, 0.8936, and 0.173, giving $K_3 = -(-0.173)/[(2)(0.836)] = 1.0 \times 10^5$ M^{-1}, essentially the same as, but slightly higher than, the value derived for Mg^{2+} present. The plot shows the cubic fit. K_3 is the same with and without Mg^{2+}, to 10% or so, which is the error in the measurement from fit of data. If $K_3 = 1.0 \times 10^5$ M^{-1}, the drug is 85% monomeric at $c_t = 1$ μM and 53% monomeric at $c_t = 8.17$ μM.

Dimethyl Sulfate Cleavage of the 18-mer. Footprinting experiments were performed for DMS/piperidine cleavage of the DNA fragment. Because cleavage by DMS takes place

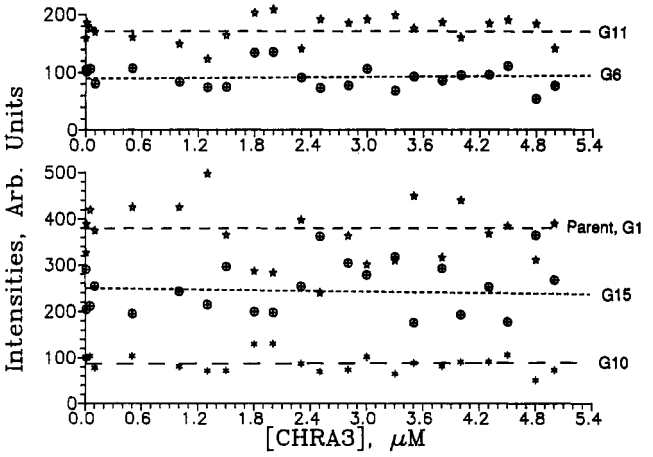

FIGURE 9: DMS/piperidine footprinting plots for the G 18-mer in the presence of various concentrations of chromomycin. Dashed curves show fits to straight lines (using all data, including intensities for drug concentrations not shown). Slopes divided by intercepts are as follows: parent band + G18, 0.0010; G6, 0.0095; G10, 0.0152; G11, –0.0019; G15, –0.0091.

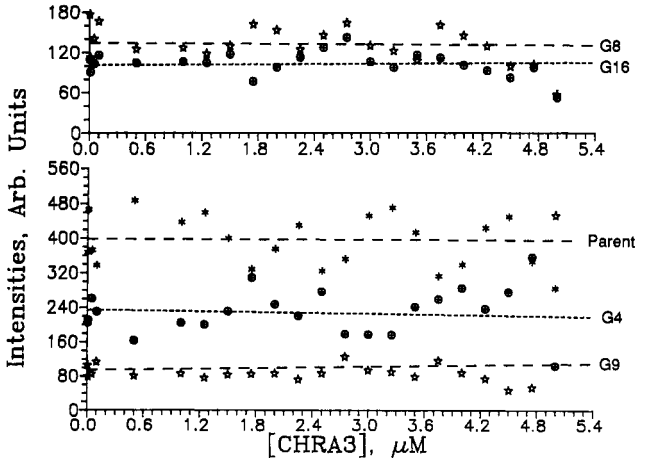

FIGURE 10: DMS/piperidine footprinting plots for the C 18-mer in the presence of various concentrations of chromomycin. Dashed curves show fits to straight lines (using all data, including intensities for drug concentration not shown). Slopes divided by intercepts are as follows: parent band, –0.0007; G16, 0.0070; G9, 0.0315; G8, –0.005; G4, –0.0116.

in the major groove by attacking N-7 of guanine (Lowley & Brookes, 1963), while chromomycin binds in the minor groove, the classic footprinting behavior (decrease of fragment intensities with drug concentration) was not expected. However, the possibility existed that bound drug, by inducing a structural change, would alter DNA cleavage rates by DMS.

For each concentration, all band intensities were divided by the total intensity to normalize them. This corrects for gel loading errors, etc., effectively giving a constant total amount of radiolabeled DNA. The normalized data for each fragment were then fitted to a linear function of drug concentration. The normalized data are shown in Figures 9 and 10 with the linear fits (broken lines). The relative slopes (slope/intercept) are close to zero in every case. Thus, no alteration in cleavage rates by drug is evidenced: the cutting rate is unaffected by drug binding.

From the NMR studies, it has been postulated that chromomycin binding alters DNA structure to A-DNA (Gao & Patel, 1989a,b, 1990; Leroy et al., 1991). This form of DNA is characterized by a wide and shallow minor groove and a narrow but deep major groove (Dickerson et al., 1982). Since changes in DNA structure have been reported to influence the alkylation rate of DMS (Nielsen, 1990), chromomycin binding to the 18-mer may affect the alkylation rates at the guanines located at positions 8–11 of the duplex. As is shown in Figure 10, the normalized bond intensities for cleavage at all guanine sites on the 18-mer labeled at C show no change in intensity as drug is added to the system. Since the DNase I footprinting studies established that drug binding is taking place, either there is no drug-induced structural change in DNA or there is a change but, under the conditions of the experiment, DMS cannot detect the change.

Implications for the Mechanism of Action of Chromomycin. It is interesting to compare the footprinting-derived binding constants with others in the literature. Behr et al. (1969) and Nayak et al. (1973) used absorption spectroscopy and Scatchard analysis to measure the binding constant of chromomycin toward calf thymus DNA. The values obtained, $(0.92–2.0) \times 10^5\ M^{-1}$, agreed with that recently measured for the related drug mithramycin using fluorescence spectroscopy. Chromomycin is also able to bind to chromatin but with a binding constant about an order of magnitude lower than for binding to calf thymus DNA (Nayak et al., 1975). While most of the reported values lie in the range $10^4–10^5\ M^{-1}$, Itzhaki et al. (1990) reported an unusually high value of $10^{11}\ M^{-1}$. This value was obtained by recording the optical changes which occur when EDTA is used to break up the chromomycin–Mg^{2+}–DNA complex in solution. The reason that our footprinting measurements return a binding constant 2 orders of magnitude higher than most other determinations is unclear. However, footprinting directly measures the fraction of a DNA site blocked by drug whereas in spectral titrations this quantity is inferred from the optical properties of the species present in solution. Since there may be a number of chromomycin species present in solution, it is dangerous to use only optical methods to measure the drug's affinity. In addition, the binding constant to calf thymus DNA is an average over many binding sites, whereas the present studies consider a fragment which is known to possess only a single strong binding site. This site is unusual in the sense that it can bind two drugs symmetrically, a situation that is not often encountered in random sequence DNA. The footprinting and fluorescence data indicate that, at the submicromolar concentration of chromomycin expected in the cell, the drug probably exists as a monomer in solution. It is unclear if the drug is complexed to ions or free in vivo. However, the high concentration of Mg^{2+} in the serum and cytoplasm suggests that a magnesium complex is likely under cellular conditions. Since most potential chromomycin binding sites on natural DNA would not have 2-fold symmetry, it would appear that monomer and not dimer binding is the mode by which the drug expresses its antitumor properties. In this regard, monomer binding can clearly be seen in the early footprinting studies by Van Dyke and Dervan (1983) using Fe-MPE as a cleavage agent. However, as has been shown in our footprinting experiments, a DNA sequence having adjacent chromomycin sites can bind two drug molecules with a binding constant 2 orders of magnitude higher than that found for other sites in random sequence DNA. Thus, dimer binding may be an important event in vivo, especially in the promoter regions of genes, which are often rich in GC content. An understanding of the form of the drug which is present in vivo is a necessary first step for understanding the drug's cytotoxic and immunosuppressive properties. Determining which of many potential binding sites in gene sequences will be bound by chromomycin will require additional study.

CONCLUSIONS

In this manuscript we show that two chromomycin A_3 molecules bind to an oligonucleotide duplex having 2-fold symmetry, with a binding constant several times 10^7 M^{-1}. The DNase I footprinting and fluorescence data show that the self-association constant for the drug outside of DNA is large, $\sim 10^5$ M^{-1}. However, at micromolar concentrations, the drug exists mainly as a monomer and binding of two drugs to the duplex takes place in a cooperative manner. Quantitative footprinting studies with dimethyl sulfate, which alkylates at N-7 of guanine located in the major groove, failed to detect a structural change in DNA in the chromomycin complex. The enhanced affinity of the drug for the 2-fold symmetric site suggests that sites of this type may be bound by drug in vivo. The results of this study, at an earlier stage of analysis, have been previously published (Dabrowiak et al., 1992).

REFERENCES

Baguley, B. C. (1982) *Mol. Cell. Biochem. 43*, 167–181.

Banville, D. L., Keniry, M. A., Kam, M., & Shafer, R. H. (1990a) *Biochemistry 29*, 6521–6534.

Banville, D. L., Keniry, M. A., & Shafer, R. H. (1990b) *Biochemistry 29*, 9294–9304.

Behr, W., Honikel, K., & Hartman, G. (1969) *Eur. J. Biochem. 9*, 82–92.

Borer, P. N. (1975) *Handbook of Biochemistry and Molecular Biology (3rd Ed.) Nucleic Acids*, Vol. 1, CRC Press, Boca Raton, FL.

Brikenshtein, V. Kh., Pitina, L. R., Barenboime, G. M., & Gurskii, G. V. (1983) *Mol. Biol. (Moscow) 18*, 1606–1616.

Chaires, J. B., Dattagupta, N., & Crothers, A. M. (1982) *Biochemistry 21*, 3927–3932.

Cons, M. G. B., & Fox, K. R. (1989a) *Nucleic Acids Res. 17*, 5447–5459.

Cons, M. G. B., & Fox, K. R. (1989b) *Biochem. Biophys. Res. Commun. 160*, 517–524.

Cons, M. G. B., & Fox, K. R. (1990) *FEBS Lett. 204*, 100–104.

Dabrowiak, J. C., Stankus, A., & Goodisman, J. (1992) *Adv. Electrophor. 5*, 113–136.

Dickerson, R. E., Drew, H. R., Conner, B. N., Wing, R. M., Fratini, A. V., & Kopka, M. L. (1982) *Science 216*, 475–485.

Fletcher, R. (1980) *Practical Methods of Optimization*, Vol. 1, John Wiley, Chichester, England.

Fox, K. R., & Howarth, N. R. (1985) *Nucleic Acids Res. 13*, 8695–8714.

Gao, X., & Patel, D. J. (1989a) *Biochemistry 28*, 751–762.

Gao, X., & Patel, D. J. (1989b) *Q. Rev. Biophys. 22*, 93–138.

Gao, X., & Patel, D. J. (1990) *Biochemistry 29*, 10940–10956.

Goodisman, J., & Dabrowiak, J. C. (1992) *Biochemistry 31*, 1058–1064.

Itzhaki, L., Weinberger, S., Livnah, & Berman, E. (1990) *Biopolymers 29*, 481–489.

Keniry, M. A., Brown, S. C., Berman, E., & Shafer, R. H. (1987) *Biochemistry 26*, 1058–1067.

Lawley, P. D., & Brookes, P. (1963) *Biochem. J. 89*, 127–128.

Leroy, J. L., Gao, X., Guéron, M., & Patel, D. (1991) *Biochemistry 30*, 5653–5661.

Miyamoto, M., Kawamatsu, Y., Kawashima, K., Shinohara, M., Tanaka, K., & Tatsuoka, S. (1967) *Tetrahedron 23*, 421–437.

Nayak, R., Sirsi, M., & Podder, S. K. (1973) *FEBS Lett. 30*, 157–162.

Nayak, R., Sirsi, M., & Podder, S. K. (1975) *Biochim. Biophys. Acta 378*, 195–204.

Nielsen, P. E. (1990) *J. Mol. Recog. 3*, 1–25.

Nielsen, P. E., Cons, B. M. G., Fox, K. R., & Vibeke, B. S. (1990) in *Molecular Basis of Specificity in Nucleic Acid–Drug Interactions* (Pullman, B., & Jortner, J., Eds.) pp 423–431, Kluwer Academic Publishers, Dordrecht, The Netherlands.

Pelton, J. G., & Wemmer, D. E. (1989) *Proc. Natl. Acad. Sci. U.S.A. 86*, 5723–5727.

Prasad, K. S., & Nayak, R. (1976) *FEBS Lett. 71*, 171–174.

Rehfuss, R., Goodisman, J., & Dabrowiak, J. C. (1990) *Biochemistry 29*, 777–781.

Sambrook, J., Fritsch, E. F., & Maniatis, T. (1989) *Molecular Cloning, A Laboratory Manual*, 2nd Ed., Cold Spring Harbor Laboratory Press, Cold Spring Harbor, NY.

Snyder, J. G., Hartman, N. G., D'Estantoit, B. L., Kennard, O., Remeta, D. P., & Breslauer, K. J. (1989) *Proc. Natl. Acad. Sci. U.S.A. 86*, 3968–3972.

Suck, D., & Oefner, C. (1986) *Nature (London) 321*, 620–625.

Tatsuoka, S., Miyake, A., & Mizuno, K. (1960) *J. Antibiot., Ser. B 13*, 332.

Van Dyke, M. W., & Dervan, P. B. (1983) *Biochemistry 22*, 2373–2377.

Ward, B., Rehfuss, R., Goodisman, J., & Dabrowiak, J. C. (1988) *Nucleic Acids Res. 16*, 1359–1369.

Ward, D. C., Reich, E., & Goldberg, I. H. (1965) *Science (Washington, D.C.) 149*, 1259–1263.